Volume 10, Issue 1, 2020, 4764 - 4773 ISSN 2069-5837
Biointerface Research in Applied Chemistry
www.BiointerfaceResearch.com
https://doi.org/10.33263/BRIAC101.764773
Original Research Article Open Access Journal
Received: 02.10.2019 / Revised: 18.11.2019 / Accepted: 20.11.2019 / Published on-line: 22.11.2019

Complexes of end-functionalized polystyrenes carrying amine end-group with transition metals: association effects in organic solvents

Paraskevi Driva [1], Marianthi Sapka [1], Anastasios Karatzas [1], Antonios Bartzeliotis [1], Linda IJsselstijn [1], Marinos Pitsikalis [1,*]

[1]Industrial Chemistry Laboratory, Department of Chemistry, National and Kapodistrian University of Athens, Panepistimiopolis Zografou, Athens, 15771, Greece
*corresponding author e-mail address: ***pitsikalis@chem.uoa.gr*** | Scopus ID 35509076100

ABSTRACT

Linear end-functionalized polystyrenes of different molecular weights bearing amino end-group (NPS) were synthesized by anionic polymerization high vacuum techniques. The polymers were exposed to copper and iron salts ($CuCl_2.2H_2O$ and $FeCl_3.6H_2O$) to form complexes with specific metal/amino molar ratios. The thermal stability of these complexes was studied by Thermogravimetric Analysis (TGA) and Differential Thermogravimetry (DTG), whereas their solution behavior was studied by Low Angle Laser Light Scattering (LALLS), Dynamic Light Scattering (DLS) and dilute solution Viscometry. Extended aggregation phenomena of these complexes were observed in organic solvents. The association behavior was influenced by the molecular weight of the polymer chain, the metal/amine group molar ratio, the chemical nature of the metal and the polarity of the solvent. A complex situation was revealed by DLS showing the existence of equilibrium between aggregates and clusters. Under the influence of shear forces applied in the capillary tube of the viscometer the clusters are disrupted.

Keywords: *end-functionalized polymers; polymer-metal complexes; association phenomena.*

1. INTRODUCTION

The ability to control the self-organization process of soft materials is the key to design and develop novel supramolecular structures with interesting properties. This is the basis of understanding the correlation between structure and dynamics in soft matter physics [1-2]. These studies include various fields of research, such as macrophase and microphase separation [3-5], gelation [6-8], crystallization [9,10] and association phenomena [11-13]. The progress in this area is closely related to the advances in the synthesis of well-defined macromolecular structures having the maximum control over the molecular characteristics and the architecture [14-22].

Polymer Chemistry has witnessed tremendous growth in recent years allowing the synthesis of tailored made macromolecules, which can interact through hydrophilic-hydrophobic effects [23-26], hydrogen bonding [27-33], ionic [34-39], thermodynamic and van der Waals forces. Of particular interest is the class of end-functionalized polymers. Significant progress has been achieved over the years in the synthesis of these materials including a remarkable variety of end-groups along with complex architectures [40]. For this purpose, several polymerization techniques have been employed. However, classical living anionic polymerization remains the first choice for the preparation of macromolecules with controlled molecular characteristics, architecture and end-group incorporation [41,42]. Over the past several years special attention has been given in the synthesis of polymers bearing dimethylamino functional end-groups and their transformation to zwitterions [43]. Linear homopolymers [44,45] and block copolymers [46-48] along with star polymers bearing different numbers of polar groups [49-54] have been previously prepared and their association behavior has been studied both in non-polar solvents and in bulk. The nature and the number of end-groups, the nature and the molecular weight of the macromolecular chain, along with the architecture are the key factors influencing the behavior in solution and in bulk.

In the present study linear semi-telechelic polystyrenes bearing amino end-groups have been prepared and employed as ligands for the complexation with Cu^{2+} and Fe^{3+}. The solution behavior of these macromolecular complexes has been studied by Low Angle Laser Light Scattering (LALLS), Dynamic Light Scattering (DLS) and dilute solution Viscometry. Extended work has been reported in the past on the complexation of polymers bearing carboxylate [55], bipyridyl [56,57], terpyridine [58] etc. groups with various metals. Of special interest is the study by Jerome et al. reporting the viscometric behavior in toluene of telechelic polyisoprenes having end-dimethylamino groups and coordinated to various transition metals [59]. The coordination ability of metal cations has been observed to be as follows: Ni<Co<Fe<Cu.

2. MATERIALS AND METHODS

2.1. Materials. The purification of the solvent (benzene), the monomer (styrene) and the polar additive (tetramethylene ethylene diamine) was accomplished according to the standards of anionic polymerization, as described in the literature [60-63]. Toluene (Aldrich 99.9%) and tetrahydrofuran, THF, (Aldrich 99.9%) were distilled from sodium after 3 hours in reflux. Methanol (99.9% Aldrich), $CuCl_2.2H_2O$ and $FeCl_3.6H_2O$ were used as received.

2.1. Synthesis of aminopolystyrenes. The synthesis of the aminopolystyrenes was accomplished by anionic polymerization high vacuum techniques. The detailed synthetic route has been described elsewhere [64,65]. The polymerization reaction of styrene was initiated with the protected amine reagent of Scheme 1 at room temperature in the presence of tetramethylene ethylene diamine (TMEDA) that was used to accelerate the initiation reaction.

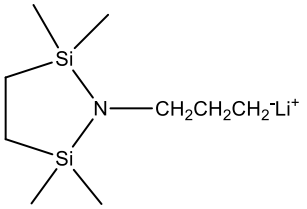

Scheme 1. Functional anionic initiator

Methanol was used as the terminating reagent of the polymerization, as well as for the deprotection of the end-amine group. The polymers were redissolved in toluene and reprecipitated in methanol several times. They were finally dried in a vacuum oven. The successful deprotection of the amine group was established with proton nuclear magnetic resonance (H^1-NMR) before and after the addition of methanol.

2.2. Preparation of the polymer-metal complexes. 2gr of an aminopolystyrene sample were dissolved in 15mls of THF. Solutions of copper chloride ($CuCl_2.2H_2O$) or iron chloride ($FeCl_3.6H_2O$) in methanol were also prepared. The appropriate amount of the methanol solution of the metal, in order to achieve specific amine/metal ratio every time, was added dropwise to the polymer solution under continuous stirring and was left at room temperature for 2-3 days. The desired amount of methanol was added and the polymer-metal complexes were left to fully precipitate for one day. The excess methanol was removed along with any excess of unreacted metal, the polymer complexes were filtered and dried in a vacuum oven overnight.

2.3. Characterization. Size Exclusion Chromatography (SEC) experiments were carried out using a modular instrument consisting of a Waters model 510 pump, U6K sample injector, 401 differential refractometer and a set of 5 μ-Styragel columns with a continuous porosity range from 500 to 10^6 Å. $CHCl_3$ was the carrier solvent at a flow rate of 1 mL/min. The system was calibrated with nine PS standards with molecular weights in the range of 970–600,000.

TGA experiments were conducted with a Q50 model from TA instruments. The heating rate was adjusted at 10 °C/min.

Static light scattering measurements were performed with a Chromatix KMX-6 low angle laser light scattering photometer at 25°C equipped with a 2 mW He-Ne laser operating at λ=633 nm. The equation (1) describing the concentration dependence of the reduced intensity is:

$$\frac{Kc}{\Delta R_\theta} = \frac{1}{M_w} + 2A_2c + \dots, \quad (1)$$

where K is a combination of optical and physical constants, including the refractive index increment, dn/dc, and the excess Rayleigh ratio of the solution over that of the solvent, ΔR_θ. Stock solutions were prepared, followed by dilution with solvent to obtain appropriate concentrations. All solutions and solvents were optically clarified by filtering through 0.22 μm pore size nylon filters directly into the scattering cell.

Refractive index increments, dn/dc, at 25°C were measured with a Chromatix KMX-16 refractometer operating at 633 nm and calibrated with aqueous NaCl solutions.

Dynamic light scattering measurements were conducted with a Series 4700 Malvern system composed of a PCS5101 goniometer with a PCS stepper motor controller, a Cyonics variable power Ar^+ laser, operating at 488 nm, a PCS8 temperature control unit, a RR98 pump/filtering unit and a 192 channel correlator for the accumulation of the data. The correlation functions were analyzed by the cumulant method and the CONTIN software. Measurements were carried out at 45°, 90° and 135°. The angular dependence of the ratio Γ/q^2, where Γ is the decay rate of the correlation function and q is the scattering vector, was not very important for most of the aggregating solutions. In these cases apparent translational diffusion coefficients at zero concentration, $D_{0,app}$ were measured using the equation (2):

$$D_{app} = D_{0,app}\left(1 + k_D c\right), \quad (2)$$

where k_D is the coefficient of the concentration dependence of the diffusion coefficient. Apparent hydrodynamic radii at infinite dilutions, R_h, were calculated by the aid of the Stokes-Einstein equation (3):

$$R_h = kT/6\pi\eta_s D_{0,app}, \quad (3)$$

where k is the Boltzmann's constant, T the absolute temperature and η_s the viscosity of the solvent.

Viscometric data were analyzed using the Huggins equation (4):

$$\frac{\eta_{sp}}{c} = [\eta] + K_H[\eta]^2 c + \dots \quad (4)$$

and the Kraemer equation (5):

$$\frac{\ln \eta_r}{c} = [\eta] + K_K[\eta]^2 c + \dots \quad (5)$$

where η_r, η_{sp} and $[\eta]$ are the relative, specific and intrinsic viscosities respectively, K_H and K_K the Huggins and Kraemer constants, respectively. All the measurements were carried out at 25°C. Cannon-Ubbelohde dilution viscometers equipped with a Schott-Geräte AVS 410 automatic flow timer were used. Viscometric radii, R_v, were calculated from the equation (6):

$$R_v = \left(\frac{3}{10\pi N_A}\right)^{1/3} \left([\eta] M_{w,app}\right)^{1/3}, \quad (6)$$

where $M_{w,app}$ is the weight average molecular weight determined by light scattering measurements.

3. RESULTS

3.1. Polymer synthesis.

The weight average molecular weights of the aminopolystyrenes were calculated by LALLS in THF, whereas their molecular weight distribution by SEC, employing $CHCl_3$ as the eluent. The data are displayed in Table 1. Well-defined polymers with low polydispersities were obtained. Furthermore,

the weight average molecular weights were similar to the stoichiometric values. These data confirm that the anionic polymerization of styrene was efficiently conducted using the functional initiator. This was further revealed by the examination of the ^{1}H NMR spectra. It was possible to calculate, by ^{1}H NMR, the M_n of the lower molecular weight sample and it was found to be in very close agreement with the LALLS measurements. These results indicate that all the PS chains are end-functionalized with the desired protected amino-group.

The deprotection reaction for the removal of the silyl protective group was performed with the treatment of the polymer with methanol in successive dissolution in toluene and precipitation in methanol steps. The success of the deprotection reaction was confirmed by ^{1}H NMR spectroscopy. The ^{1}H-NMR spectra before and after the deprotection of the amine group of the aminopolystyrenes are given in Figures SI1a and SI1b respectively of the Supporting Information Section (SI). The peaks in Figure SI1a between 0 and 1 ppm, attributed to protons of the protective group, have disappeared in Figure SI1b after treatment with methanol, revealing quantitative deprotection.

The aminopolystyrenes were dissolved in THF and mixed with either $CuCl_2.2H_2O$ or $FeCl_3.6H_2O$ in MeOH. Both solvents were selected due to their high polarity that would ensure complete dissolution of the polymers as well as the metal salts. Since methanol is not a good solvent for the aminopolystyrenes the amount mixed with the polymer solution was very small to avoid the polymer precipitation. Samples are symbolized as NPS, indicating the aminopolystyrene sample, followed by the molecular weight of the chain, the metal complexed with the polymer amino groups, either Cu or Fe and finally the metal/amine molar ratio. For example NPS-8-Cu-0.25 refers to a complex of the aminopolystyrene with molecular weight 8100 complexed with Cu using a metal/amine molar ratio of 1/4.

Table 1. Molecular characteristics of the aminopolystyrenes

Sample	M_w x 10^{-3} [a]	A_2 x 10^3 mL·mol·g^{-2}	M_w/M_n [b]
NPS8	8.1	8.30	**1.13**
NPS28	**28.3**	**3.04**	**1.06**

[a] By low angle laser light scattering (LALLS) in THF at 25 °C.
[b] By size exclusion chromatography (SEC) in $CHCl_3$.

3.2. Thermal stability of the complexes.

The thermal stability of the complexes was studied by Thermogravimetric Analysis, TGA, and Differential Thermogravimetry, DTG. The homopolymer NPS-8 was initially studied as a reference and then the complexes NPS-8-Fe and NPS-8-Cu as representative examples. The results are listed in Table 2, whereas characteristic decomposition patterns are provided in Figure 1.

Compared to the amino-functionalized homopolymer NPS-8 the complexes present similar simple one step decomposition profiles, however with the following differences:

a. The temperature, where the maximum rate of thermal decomposition was observed, was slightly increased in the complexes.
b. The temperature range for the thermal decomposition of the complexes was substantially increased.
c. Negligible residue was found after the thermal decomposition of the NPS-8 sample, whereas residue, up to 1% was found in the case of the complexes, due to the remaining metal compounds after the thermal treatment.

These results confirm the formation of the polymeric complexes and indicate that the presence of the metal improves the thermal stability of the polymeric materials.

Table 2. TGA results of the polymer metal complexes.

Sample	Maximum Temperature of Thermal Decomposition, °C	Temperature Region of Thermal Decomposition, °C	Residue %
NPS-8	425.88	362.93-462.27	**0.00**
NPS-8-Fe-0.25	427.83	365.49-483.78	**0.46**
NPS-8-Fe-0.50	427.03	361.67-475.90	**0.84**
NPS-8-Fe-1.00	428.30	368.33-477.16	**0.89**
NPS-8-Fe-1.25	428.45	368.33-472.76	**0.93**
NPS-8-Cu-0.25	427.09	369.44-476.10	**0.52**
NPS-8-Cu-0.50	431.00	369.44-474.99	**0.92**
NPS-8-Cu-1.00	433.03	370.55-477.21	**0.57**
NPS-8-Cu-1.25	**436.57**	**365.00-478.32**	**1.00**

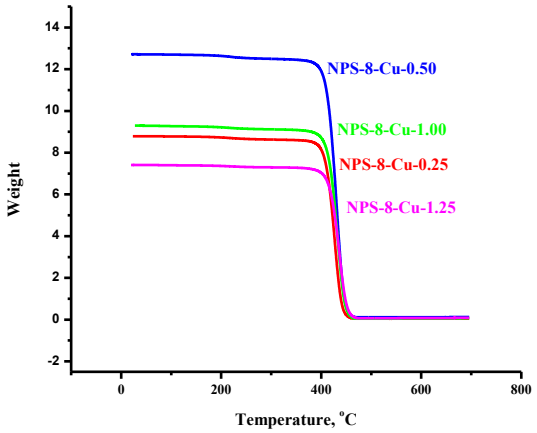

Figure 1. Thermal degradation curves from TGA for the NPS-8-Cu complexes.

3.2. LALLS measurements.

The results from low-angle laser light scattering (LALLS) in the non polar solvent toluene are given in Tables 3 and 4 for the complexes obtained from NPS8 and NPS28, respectively. Characteristic $Kc/\Delta R_\theta$ vs c plots are displayed in Figure 2, whereas more plots are incorporated in the SI. The aggregation numbers (N_w), defined as the ratio of the weight-average molecular weight of the polymer complexes in toluene over that of the NPS samples in THF, are shown in Tables 3 and 4.

Table 3. LALLS results for the NPS8-Cu and NPS8-Fe Complexes in Toluene at 25 °C.

Metal/Amine Ratio	Sample	M_wx10^{-5} g·mol^{-1}	A_2x10^5 mL·mol·g^{-2}	N_w [a]
0.25	NPS8-Fe-0.25	28.4	21.3	**351**
	NPS8-Cu-0.25	2.66	1.22	**33**
0.5	NPS8-Fe-0.5	15.3	4.80	**189**
	NPS8-Cu-0.5	27.0	0.94_4	**333**
1.0	NPS8-Fe-1.0	16.4	17.8	**202**
	NPS8-Cu-1.0	20.0	-4.19	**247**
1.25	NPS8-Fe-1.25	16.7	3.73	**207**
	NPS8-Cu-1.25	**9.20**	**19.5**	**113**

[a] Weight average degree of association.

Table 4. LALLS results for the NPS28-Cu and NPS28-Fe Complexes in Toluene at 25 °C

Metal/Amine Ratio	Sample	$M_w x10^{-4}$ g·mol^{-1}	$A_2 x10^4$ mL·mol·g^{-2}	N_w[a]
0.25	NPS28-Fe-0.25	22.2	-8.95	**8**
	NPS28-Cu-0.25	2.56	3.43	**1**
0.5	NPS28-Fe-0.5	22.9	0.30_3	**8**
	NPS28-Cu-0.5	21.0	7.10	**7**
1.0	NPS28-Fe-1.0	83.1	1.70	**29**
	NPS28-Cu-1.0	3.88	18.3	**1**
1.25	NPS28-Fe-1.25	28.2	-0.78_5	**10**
	NPS28-Cu-1.25	—	—	—

[a] Weight average degree of association

It is evident that aggregates exist in toluene solutions of the complexes of the aminopolymers with the metal salts, as a result of the increased weight average molecular weights of the polymer complexes in toluene compared to the polymer precursors prior the complexation process. The polar metal centers of the complexes are not soluble in toluene resulting in aggregation phenomena in order to prevent the interactions of the metal atoms with the non polar solvent. The complexes that were prepared after the exposure of NPS8 to metal salts have higher molecular weights than those from NPS28. This is due to excluded volume effects, which are more intense when higher molecular weight polymer chains are employed. The lower molecular weight chains can be accommodated easier around the metal center, due to weaker steric hindrance effects. When the precursor polymer has low molecular weight the chains are capable of getting closer to each other and creating bigger aggregates in size. On the contrary, when the precursor polymer has high molecular weight, due to the excluded volume effect, the tendency to aggregate and protect the metal atoms is encumbered resulting in lower weight average degrees of association. Another reason is that higher molecular weight polymer chains are capable to dilute more effectively the metal centers so there is no need for high degrees of aggregation.

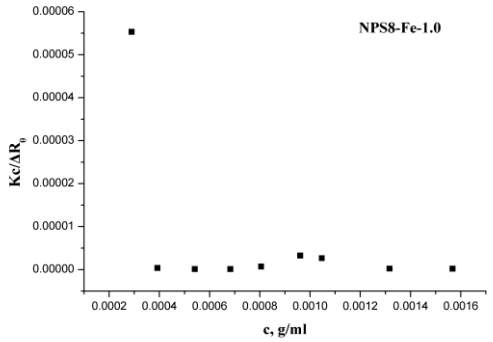

Figure 2. LALLS plot for sample NPS-8-Fe-1.0 in toluene

In addition, A_2 values of the NPS complexes in toluene are significantly lower than those of the precursor aminopolystyrenes in the same solvent and in some cases they even present negative numbers. Since A_2 expresses the thermodynamic interactions between polymer chains and solvent molecules a decrease of this factor is indicative of the presence of aggregates in the system. Aggregation results in increasing interactions between polymer chains and thereby decreasing the value of the second virial coefficient for the complexes' solutions.

It is interesting to study the dependence of the aggregation numbers with the metal/amine ratio. For the NPS8-Fe samples a maximum N_w value was observed for sample NPS8-Fe-0.25, whereas the NPS28-Fe samples the maximum N_w value was observed for sample NPS28-Fe-1.0. The polymeric metal complexes with the other metal/amine ratios showed more or less similar aggregation numbers. This is a direct indication that in the case of the low molecular weight sample four NPS chains interact with the Fe center, whereas in the case of the higher molecular weight sample only one chain interacts with the Fe center, obviously due to the extended excluded volume effects. For the Cu series, the maximum value of the degree of association is observed at a metal/amine ratio equal to 0.5 for both aminopolystyrenes showing that the complexing ability of the metal center greatly affects the association behavior. It is obvious that slightly stronger aggregation is observed in the presence of Fe than Cu. The aggregation behavior will be further explored by Dynamic Light Scattering and dilute solution viscometry experiments.

3.3. Dynamic Light Scattering measurements.

The static light scattering results were further confirmed by dynamic light scattering (DLS). Measurements were conducted in 45º, 90º and 135º angles where diffusion coefficient D_0, k_D factor, as well as the hydrodynamic radius R_h were calculated for each sample. Results in 90º angle concerning NPS8 and NPS28 complexes are displayed in Table 5 and 6, respectively. The concentration dependence of the apparent diffusion coefficient was linear for almost all samples. Representative plots are given in Figure 3. More examples are included in the SI.

Table 5. DLS results for the NPS8-Cu and NPS8-Fe Complexes in Toluene at 25 °C.

Metal/Amine Ratio	Sample	$D_0 x10^8$ cm^2·s^{-1}	k_D mL·g^{-1}	R_h nm
	NPS8	—	—	**1.87**[a]
0.25	NPS8-Fe-0.25	4.04	269.4	**97.8**
	NPS8-Cu-0.25	5.73	-5.90	**69.1**
0.5	NPS8-Fe-0.5	15.4	-292.0	**25.7**
	NPS8-Cu-0.5	4.88	-28.0	**81.0**
1.0	NPS8-Fe-1.0	7.54	-38.1	**53.1**
	NPS8-Cu-1.0	5.67	-10.9	**69.8**
1.25	NPS8-Fe-1.25	4.49	34.4	**88.0**
	NPS8-Cu-1.25	**7.23**	**29.5**	**54.7**

[a].Calculated from the theoretical equation $R_h^{TOLUENE} = 1.06 \times 10^{-2} M^{0.575}$ from literature.

It is obvious that there is a clear difference between R_h values of the complexes and those of the precursor aminopolystyrenes. These results are in agreement with the results from LALLS, where the molecular weight of the complexes increased tremendously due to extended aggregation phenomena. Angular dependence of R_h was observed for all samples, indicating that the shape of the aggregates was not spherical. In addition to increased R_h values of the complexes, most of the k_D values are negative. From the equation $k_D=2A_2M-k_f-u_2$, where the factor $2A_2M$ is associated with thermodynamic interactions and k_f with hydrodynamic ones, assures that k_D is related to the second virial coefficient, A_2. A decrease in polymer-solvent interactions, due to aggregation phenomena, results in low A_2 values and thus negative k_D.

Generally, for NPS8-Fe complexes (Table 5), a maximum R_h value is observed for metal/amine ratio equal to 0.25, in which ratio the degree of association also receives the maximum value. With the exception of sample NPS8-Fe-0.25, R_h increases upon increasing the metal/amine ratio. The hydrodynamic radius of NPS8-Fe-0.5 as well as of NPS28-Fe-0.5 (Table 6) is much lower than those of the rest of the samples of each series. Since the molecular weights do not differ that much the above observation indicates that the formed aggregates have very compact structures. In addition, these samples have also highly negative values of k_D, which reflects reduced hydrodynamic interactions of the aggregates with the solvent. On the contrary, the NPS8-Cu complexes, displayed an opposite behavior with the R_h values decreasing upon increasing the metal/amine ratio, as was also observed for the N_w values. The maximum R_h and N_w values were obtained for the same metal/amine molar ratio, equal to 0.5 for this series of complexes.

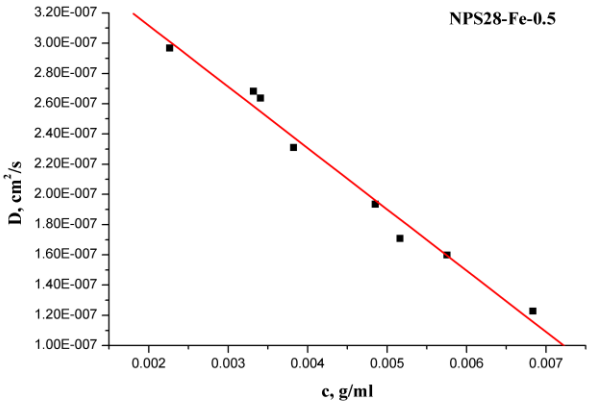

Figure 3. DLS plot for sample NPS-28-Fe-0.5 in toluene.

Table 6. DLS results for the NPS28-Cu and NPS28-Fe Complexes in Toluene at 25°C

Metal/Amine Ratio	Sample	$D_o x10^8$ $cm^2 \cdot s^{-1}$	k_D $mL \cdot g^{-1}$	R_h nm
	NPS28	—	—	**3,84**[a]
0.25	NPS28-Fe-0.25	6.40	271.7	**61.8**
	NPS28-Cu-0.25	13.4	239.2	**29.6**
0.5	NPS28-Fe-0.5	39.3	-103.9	**9.8**
	NPS28-Cu-0.5	15.4	33.9	**25.6**
1.0	NPS28-Fe-1.0	5.66	17.6	**69.9**
	NPS28-Cu-1.0	5.68	196.0	**69.6**
1.25	NPS28-Fe-1.25	4.40	79.8	**89.8**
	NPS28-Cu-1.25	—	—	—

[a] Calculated from the theoretical equation $R_h^{TOLUENE} = 1.06 \times 10^{-2} M^{0.575}$ from literature

CONTIN analysis for the NPS8 series confirmed the presence of two peaks, meaning that two different populations exist in the solutions. In the case of the NPS8-Fe complexes, taking into account the molecular weight of the precursor, these populations are attributed to aggregates and clusters, due to their very large hydrodynamic radii. The two populations are better resolved in more concentrated solutions, where the composition in clusters becomes higher, up to 50% by intensity. The same trend is observed as the Fe/amine molar ratio increases, where no free chains were traced. The polydispersity factor μ_2/Γ^2, where Γ is the decay rate of the correlation function and μ_2 the second moment of the cumulant analysis, is always higher than 0.2, indicating the presence of polydisperse structures. For NPS8-Cu complexes the existence of clusters is not as extensive. In low concentrations and/or low Cu/amine ratios one rather monodisperse peak (μ_2/Γ^2<0.2) is observed, while in higher concentrations and especially for Cu/amine ratios 1.0 and 1.25 there are two peaks in 50% composition each (at 50 nm and 180 nm, respectively). Also in this case, the population with the smaller size is attributed to aggregates, whereas the bigger one to clusters of aggregates. The increase of concentration in all samples seems neither to change the composition of those populations nor their polydispersity, but increases their apparent radius.

For NPS28-Fe complexes (Table 6), except NPS28-Fe-0.5, the formed structures are characterized by a high hydrodynamic radius, even though degrees of association were low, as indicated from LALLS measurements. Furthermore, for NPS28-Cu complexes, R_h increases with increasing of metal/amine ratio, a tendency which is opposite to that observed for the low molecular weight aminopolystyrene. CONTIN analysis for NPS28-Fe complexes showed two populations, according to the molecular weights calculated, which are attributed to aggregates with lower and higher degree of association and not to clusters. Again, increase in the concentration of the solutions and in Fe/amine ratio results in good segregation of the two populations "moving" the equilibrium towards the higher molecular weight population. The samples NPS28-Cu showed one unimolecular peak (μ_2/Γ^2< 0,1) in 90% composition and ~15 nm size, which is attributed to slightly aggregated aminopolystyrene complexes and the second peak in 10% composition and ~150 nm size , having polydispersity higher than 0,2 which is attributed to clusters. Again in this case we come to the conclusion that polymer chains with higher molecular weight dilute the polar metal atoms more effectively than the low molecular weight ones forming smaller aggregates in size.

As shown by the CONTIN analysis in all cases there was no population with hydrodynamic radius of free chains, which reinforces the view that there were no chains without amino groups, which could not be complexed to the metal center. To exclude the fact that the amino group has no role in complexation, DLS measurements were performed on standard polystyrenes (PS) in the presence of iron salt. Molecular characteristics of PS and DLS data were given in Table 7.

Table 7. Molecular Characteristics and DLS results for standard polystyrenes in Toluene at 25 °C in the presence of iron salt.

Sample	$M_w x10^{-3}$	$D_o x10^8$ $cm^2 \cdot s^{-1}$	k_D $mL \cdot g^{-1}$	R_h nm
PS14	14.0	35.8	147.4	**11.8**
PS30	**30.0**	**48.7**	**98.9**	**9.7**

No angular or concentration dependence of R_h was observed for the two samples. By CONTIN analysis only one monodisperse population was existed with very low R_h values compared to the NPS samples ones. From these results can be concluded that the amino group is responsible for the complexation of polymer chains, which occurs after the treatment of polymer solutions with metal ions.

In the series of NPS8-Fe complexes, DLS measurements were carried out in THF to study the effect of polarity of the

solvent in aggregate formation. The results are displayed in the comparative Table 8.

Table 8. Dependence of aggregation on solvent polarity. DLS results for the NPS8-Fe Complexes in Toluene and THF at 25 °C

	TOLUENE			THF		
Sample	**D_0x10^8 $cm^2 \cdot s^{-1}$**	**k_D $mL \cdot g^{-1}$**	**R_h nm**	**D_0x10^8 $cm^2 \cdot s^{-1}$**	**k_D $mL \cdot g^{-1}$**	**R_h nm**
NPS8-Fe-0.25	4.04	269.4	97.8	12.1	42.3	**39.2**
NPS8-Fe-0.5	15.4	-292.0	25.7	8.60	-74.3	**55.19**
NPS8-Fe-1.0	7.54	-38.1	53.1	14.4	-72.1	**32.94**
NPS8-Fe-1.25	**4.49**	**34.4**	**88.0**	**11.0**	**4.3×10^{-2}**	**43.12**

There is a clear difference between the results of NPS8-Fe samples in toluene and in THF. The diffusion coefficient is generally higher for the samples dissolved in THF and more importantly, the R_h values of the samples in THF are much lower than those in toluene. This is a reasonable outcome since THF is a more polar solvent than toluene. Therefore it can better solubilize the metal ions leading to lower aggregation numbers. In the case of NPS8-Fe-0.5 sample the opposite trend is found and hydrodynamic radius is bigger in THF than in toluene. The aggregates may be swollen by THF, since it is a better solvent for the formed complexes and can expand the corona of the aggregates.

3.4. Viscometry measurements.

Viscometry measurements were conducted in toluene for all samples at 25^0C and confirmed the presence of aggregates. Results for NPS8 and NPS28 complexes, as well as for precursor aminopolystyrenes, are cited in Table 9 and Table 10, correspondingly. Viscometric radii, R_v, were calculated from the following equation:

$$R_v = \left(\frac{3}{10\pi N_A}\right)^{1/3} \left([\eta] M_{w,app}\right)^{1/3},$$

where $M_{w,app}$ is the weight average molecular weight determined by light scattering measurements. Representative plots are displayed in Figure 4. More data are given in the SI.

The existence of aggregates in the presence of metal ions is confirmed from the increased R_v values in toluene, compared to those obtained in the same solvent for the aminopolystyrenes. The high values of the Huggins coefficients, due to increased hydrodynamic interactions of the polymeric chains in the aggregates, lead to the same conclusion.

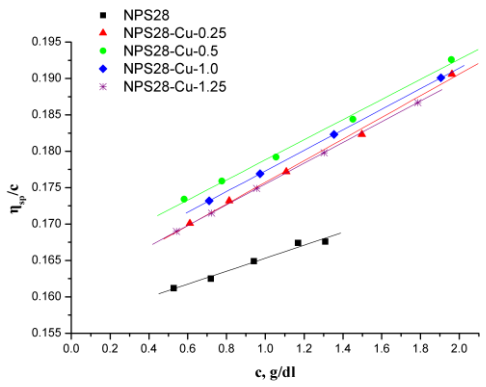

Figure 4. Huggins plots for samples NPS-28-Cu in toluene.

Table 9. Viscometry results for the NPS8-Cu and NPS8-Fe Complexes in Toluene at 25 °C.

Metal/Amine Ratio	Sample	[η] $dL \cdot g^{-1}$	k_H	R_v nm
	NPS8	0.099	0.38	**2.3**
0.25	NPS8-Fe-0.25	0.108	0.56	**16.9**
	NPS8-Cu-0.25	0.101	1.95	**7.5**
0.5	NPS8-Fe-0.5	0.106	0.72	**13.7**
	NPS8-Cu-0.5	0.102	3.12	**16.3**
1.0	NPS8-Fe-1.0	0.109	0.56	**14.1**
	NPS8-Cu-1.0	0.113	0.77	**15.3**
1.25	NPS8-Fe-1.25	0.107	0.61	**14.1**
	NPS8-Cu-1.25	**0.114**	**0.53**	**11.8**

Table 10. Viscometry results for the NPS28-Cu and NPS28-Fe Complexes in Toluene at 25 °C.

Metal/Amine Ratio	Sample	[η] $dL \cdot g^{-1}$	k_H	R_v nm
	NPS28	0.156	0.36	**4.1**
0.25	NPS28-Fe-0.25	0.163	0.63	**8.3**
	NPS28-Cu-0.25	0.161	0.58	**4.0**
0.5	NPS28-Fe-0.5	0.154	0.67	**8.2**
	NPS28-Cu-0.5	0.165	0.51	**8.2**
1.0	NPS28-Fe-1.0	0.167	0.49	**13.0**
	NPS28-Cu-1.0	0.163	0.53	**4.6**
1.25	NPS28-Fe-1.25	0.161	0.56	**9.0**
	NPS28-Cu-1.25	**0.161**	**0.55**	—

It is observed that the R_v values are always lower than the corresponding R_h values, as calculated from DLS measurements. This behavior can be attributed to the higher sensitivity of dynamic light scattering to the larger in size structures (D is a z-average quantity) and/or the development of shear forces in the capillary viscometer which may disrupt the aggregates. This behavior has been previously obtained in micellar and aggregating systems [66]. This may be also the reason why all the complexes in the same series have approximately similar intrinsic viscosities [η], regardless of metal ion and metal/amine ratio. Viscometric radii are much higher for NPS8 than NPS28 series, although intrinsic viscosities values are lower in the former case. This arises from increased values of weight average molecular weight determined by light scattering measurements. In this case also, R_vs are independent of the type of metal ion and metal/amine ratios. Especially, for NPS28-Cu-0.25 and NPS28-Cu-1.0 samples R_vs are the same with the precursor aminopolystyrene but k_H display increased values because of the tendency of polymer chains to aggregate.

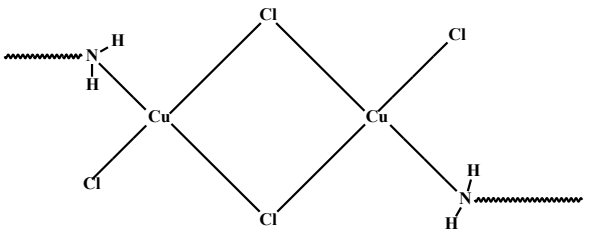

Scheme 2. Proposed structures of the polymer complexes.

Viscometry measurements made for the NPS8-Fe complexes in THF at 25 °C lead to the same conclusion. According to the comparative results in Table 11, intrinsic viscosities values of NPS8-Fe complexes into the more polar solvent THF are equal to the precursor aminopolystyrene. On the

contrary Huggins coefficients are much higher due to the hydrodynamic interactions of the polymeric chains. In THF, the secondary interactions, which are responsible for the formation of aggregates, are wicker and shear forces applied in the capillary viscometer split the complexed chains effectively leading to [η] values corresponding to the diluted chains.

All the data given above indicate a very complex association behavior of the polymer metal complexes in solutions. It is obvious that a hierarchical organization is observed. Initially, the amine-functionalized polymers form complexes with the metal atoms through the function of the amine groups as σ-donors to the coordination sphere of the metal. These metal complexes associate in non-polar solvents forming aggregates and finally, these aggregates are further organized to clusters. The angular dependence in DLS, especially for the low molecular weight sample, NPS-8, indicates the presence of non-spherical structures. The rather low values of intrinsic viscosities indicate that most probably the clusters and the aggregates, to a lesser extent, are not very stable under the application of the shear forces in the capillary tube. Therefore, under the dilute solution viscometry measurements mainly the pure metal complexes are present. For almost all cases the metal/amine ratio, where the highest [η] value was obtained was equal to one. This leads us to the conclusion that the most probable structure of the metal complexes is the one given in Scheme 2. This result is in agreement with the conclusions drawn by Jerome et al. who studied the viscometric behavior in toluene of telechelic polyisoprenes having end-dimethylamino groups and coordinated to various transition metals [59].

Table 11. Viscometry results for the NPS8-Fe complexes in THF and toluene at 25°C

	TOLUENE			THF	
Sample	**[η] dL·g^{-1}**	**k_H**	**R_v nm**	**[η] dL·g^{-1}**	**k_H**
NPS8	0.099	0.38	2.3		
NPS8-Fe-0.25	0.108	0.56	16.9	0.099	**0.77**
NPS8-Fe-0.5	0.106	0.72	13.7	0.099	**0.66**
NPS8-Fe-1.0	0.109	0.56	14.1	0.101	**0.56**
NPS8-Fe-1.25	**0.107**	**0.61**	**14.1**	**0.099**	**0.62**

4. CONCLUSIONS

Anionic polymerization high vacuum techniques were employed for the synthesis of linear end-functionalized polystyrenes having amino end-group (NPS). These polymers were further served as ligands for the synthesis of complexes with Cu and Fe. Thermogravimetric Analysis (TGA) and Differential Thermogravimetry (DTG) revealed that these complexes are thermally more stable than the parent polymeric ligands. The solution behavior of these complexes was studied by Low Angle Laser Light Scattering (LALLS), Dynamic Light Scattering (DLS) and dilute solution Viscometry. It was found that extended aggregation phenomena exist in organic solvents. The association behavior was influenced by the molecular weight of the polymer chain, the metal/amine group molar ratio, the chemical nature of the metal and the polarity of the solvent. A complex situation was revealed by DLS showing the existence of equilibrium between aggregates and clusters. Under the influence of shear forces applied in the capillary tube of the viscometer the clusters are disrupted. As a result of these findings, a hierarchical organization is obvious starting from the complexes with the polymeric ligands, then to aggregates of these complexes in non-polar solvents and finally to clusters of these initial aggregates upon increasing the concentration.

5. REFERENCES

1. Hamley, I.W. *The physics of block copolymers*. Oxford Science Publications; **1998**.
2. Zhou, L. *Introduction to soft matter physics*. World Scientific, **2019**.
3. Hamley, I.W. (ed) *Developments in block copolymer science and technology.* John Wiley & Sons, Ltd., **2004;** https://doi.org/10.1002/0470093943.
4. Rumyantsev, A.M.; Kramarenko, E.Y. Two regions of microphase separation in ion-containing polymer solutions. *Soft Matter*, **2017**, *13*, 6831-6844, https://doi.org/10.1039/C7SM01340J.
5. Horn, J.M.; Kapelner, R.A.; Obermeyer, A.C. Macro- and Microphase Separated Protein-Polyelectrolyte Complexes: Design Parameters and Current Progress. *Polymers* **2019**, *11*, 1-26, https://doi.org/10.3390/polym11040578.
6. Almgren, M.; Brown, W.; Hvidt, S. Self-aggregation and phase behavior of poly(ethylene oxide)-poly(propylene oxide)-poly(ethylene oxide) block copolymers in aqueous solution. *Colloid Polym. Sci.* **1995**, *273*, 2-15, https://doi.org/10.1007/BF00655668.
7. Hvidt, S.; Jørgensen, E.B.; Schillén, K.; Brown, W. Micellization and Gelation of Aqueous Solutions of a Triblock Copolymer Studied by Rheological Techniques and Scanning Calorimetry. *J. Phys. Chem.* **1996,** *98,* 12320-12328, https://doi.org/10.1021/j100098a030.
8. Wanka, C.; Hoffmann, H.; Ulbricht, U. Phase Diagrams and Aggregation Behavior of Poly(oxyethylene)-Poly(oxypropylene)-Poly(oxyethylene) Triblock Copolymers in Aqueous Solutions. *Macromolecules* **1994**, *27*, 4145-4159, https://doi.org/10.1021/ma00093a016.
9. Müller, A.J.; Balsamo, V.; Arnal, M.L. Nucleation and crystallization in diblock and triblock copolymers. *Adv. Polym. Sci.* **2005**, *190*, 1-63 DOI 10.1007/12_001.
10. Zhang, M.C.; Guo, B.H.; Xu, J. A review on polymer crystallization theories. *Crystals* **2017**, *7*, 1-37, https://doi.org/10.3390/cryst7010004.
11. Wakaskar, R.R. Polymeric Micelles and their Properties. *J. Nanomed. Nanotechnol.* **2017**, *8*, 433-434, https://doi.org/10.4172/2157-7439.1000433.
12. Alves, V.M.; Hwang, D.; Muratov, E.; Sokolsky-Papkov, M.; Varlamova, E.; Vinod, N.; Lim, C.; Andrade, C.H.; Tropsha, A.; Kabanov, A. Cheminformatics-driven discovery of polymeric micelle formulations for poorly soluble drugs. *Sci. Adv.* **2019**, *5*, 1-13, https://doi.org/10.1126/sciadv.aav9784.
13. Chen, L.; Lee, H.-S.; Lee, S. Close-packed block copolymer micelles induced by temperature quenching. PNAS **2018**, 7218-7223, https://doi.org/10.1073/pnas.1801682115.
14. Hadjichristidis, N.; Hirao, A.; Tezuka, Y.; Du Prez, F. *Complex macromolecular architectures. Synthesis, characterization, self-assembly.* John Wiley & Sons (Asia) Pte, Ltd. **2011**; https://doi.org/10.1002/9780470825150.

15. Pitsikalis, M.; Pispas, S.; Mays, J.W.; Hadjichristidis, N. Non-linear block copolymer architectures Adv. Polym. Sci. **1998**, *135*, 1-137, https://doi.org/10.1007/3-540-69191-X_1.
16. Hadjichristidis, N.; Pitsikalis, M.; Iatrou, H.; Pispas, S. The Strength of the Macromonomer Strategy for Complex Macromolecular Architecture. Molecular Characterization, Properties and Applications of Polymacromonomers *Macromol. Rapid Comm.* **2003,** *24*, 979-1013, https://doi.org/10.1002/marc.200300050.
17. Hadjichristidis, N.; Iatrou, H.; Pitsikalis, M.; Mays, J.W. Macromolecular architectures by living and controlled/living polymerizations S, Misra RDK The significance of macromolecular architecture. *Progr. Polym. Sci.* **2006**, *31*, 1068-1132, https://doi.org/10.1016/j.progpolymsci.2006.07.002.
18. Patil, S. Governing structure-property relationship for biomaterial applications: an overview. *Mater. Technol. Adv. Perform. Mater.* **2018**, *33*, 364-386, https://doi.org/10.1080/10667857.2018.1447266.
19. Nikovia, C.; Theodoridis, L.; Alexandris, S.; Bilalis, P.; Hadjichristidis, N.; Floudas, G.; Pitsikalis, M. Macromolecular brushes by combination of ring-opening and ringopening metathesis polymerization. Synthesis, self-assembly, thermodynamics and dynamics. *Macromolecules* **2018**, *51*, 8940-8955, https://doi.org/10.1021/ acs.macromol.8b01905
20. Bačová, P.; Foskinis, R.; Glynos, E.; Rissanou, A.N.; Anastasiadis. S.H.; Harmandaris, V. Effect of macromolecular architecture on the self-assembly behavior of copolymers in a selective polymer host. *Soft Matter*, **2018**, *14*, 9562-9570, https://doi.org/10.1039/C8SM01421C.
21. Mikhailov, I.V.; Leermakers, F.A.M.; Borisov, O.V.; Zhulina, E.B.; Darinskii, A.A.; Birshtein, T.M. Impact of Macromolecular Architecture on Bending Rigidity of Dendronized Surfaces *Macromolecules* **2018**, *519,* 3315-3329 https://doi.org/10.1021/acs.macromol.7b02400.
22. Kanso, M.A.; Giakomin, A.J.; Saengow, C.; Piette. J.H. Macromolecular architecture and complex viscosity. *Physics of Fluids* **2019,** *31*, 087107; https://doi.org/10.1063/1.5111763.
23. Sarkar, R.; Gowd, E.B.; Ramakrishnan, S. De-symmetrizing periodically grafted amphiphilic copolymers: design, synthesis and generation of Janus folded chains. *Polym. Chem.* **2019**, *10*, 1730-1740, https://doi.org/10.1039/C9PY00047J.
24. Xu, X.; Zhang, Q.; Liu, K.; Liu, N.; Han, Y.; Chen, W.; Xie, C.; Li, P.; He, J. Photo-controlled release of metal ions using triazoline-containing amphiphilic copolymers. *Polym. Chem.* **2019**, *10*, 3585-3596, https://doi.org/10.1039/C9PY00406H.
25. Zheng, K.; He, J. Amphiphilic Dendrimer-like Copolymers with High Chain Density by Living Anionic Polymerization. *Chin. J. Polym. Sci.* **2019**, *37*, 875-883, https://doi.org/10.1007/s10118-019-2247-7.
26. Mitsoni, E.; Roka, N.; Pitsikalis, M. Statistical copolymerization of N-vinyl-pyrrolidone and alkyl methacrylates via RAFT: reactivity ratios and thermal analysis *J. Polym. Res.* **2019**, *26*, *118,* 1-12, https://doi.org/10.1007/s10965-019-1776-7.
27. Sijbesma, R.P.; Meijer, E.W. Self-assembly of well-defined structures by hydrogen bonding. *Curr. Opin. Coll. Inter. Sci.,* **1999**, *4*, 24-32, https://doi.org/10.1016/S1359-0294(99)00011-4.
28. Liu, C.Z.; Yan, M.; Wang, H.; Zhang, D.W.; Li, Z.T. Making Molecular and Macromolecular Helical Tubes: Covalent and Noncovalent Approaches *ACS Omega* **2018**, *3*, 5165-5176 https://doi.org/10.1021/acsomega.8b00681.
29. Liu, T.; Peng, X.; Chen, Y.-N.; Bai, Q.-W.; Shang C.; Zhang, L.; Wang H. Hydrogen-Bonded Polymer–Small Molecule Complexes with Tunable Mechanical Properties. *Macromol. Rapid Commun.* **2018**, *39*, 1800050 (1-7), https://doi.org/10.1002/marc.201800050.
30. Schmuck, C.; Wienand, W. Self-Complementary Quadruple Hydrogen-Bonding Motifs as a Functional Principle: From Dimeric Supramolecules to Supramolecular Polymers. *Angew. Chem. Int. Ed. Engl.* **2001**, *40*, 4363-4369, https://doi.org/10.1002/1521-3773(20011203)40:23<4363::AID-ANIE4363>3.0.CO;2-8.
31. Yang, X.; Hua, F.; Yamato, K.; Ruckenstein, E.; Gong, B.; Kim, W.; Ryu, C.Y. Supramolecular AB Diblock Copolymers. *Angew. Chem. Int. Ed.* **2004**, *43*, 6471-6474, https://doi.org/10.1002/anie.200460472.
32. Binder, W.H.; Bernstorff, S.; Kluger, C.; Petraru, L.; Kunz, M.J. Tunable Materials from Hydrogen-Bonded Pseudo Block Copolymers, *Adv. Mater.* **2005**, *17* 2824-2828, https://doi.org/10.1002/adma.200501505.
33. Tee, H.T.; Koyonov, K.; Reichel, T.; Wurm, F.R. Noncovalent Hydrogen Bonds Tune the Mechanical Properties of Phosphoester Polyethylene Mimics *ACS Omega* **2019**, *4*, 9324–9332, https://doi.org/10.1021/acsomega.9b01040.
34. Gohy, J.C.; Lohmeijer, B.G.G.; Schubert, U.S. From supramolecular block copolymers to advanced nano-objects. *Chem. Eur. J.* **2003**, *9*, 3472-3479, https://doi.org/10.1002/chem.200204640.
35. Gohy, J.C.; Lohmeijer, B.G.G., Alexeev, A.; Wang, X.-S.; Manners, I.; Winnik, M.A.; Schubert, U.S. Cylindrical Micelles from the Aqueous Self-Assembly of an Amphiphilic Poly(ethylene oxide)-b-Poly(ferrocenylsilane) (PEO-b-PFS) Block Copolymer with a Metallo-Supramolecular Linker at the Block Junction. *Chem. Eur. J.* **2004**, *10* 4315-4323. https://doi.org/10.1002/chem.200400222;
36. Gohy, J.C., Lohmeijer, B.G.G.; Schubert, U.S. Metallo-Supramolecular Block Copolymer Micelles. *Macromolecules* **2002**, *35* 4560-4563, https://doi.org/10.1021/ma012042t.
37. J.C. Gohy, B.G.G. Lohmeijer, S.K. Varshney, U.S. Schubert, Covalent vs Metallo-supramolecular Block Copolymer Micelles. *Macromolecules* **2002**, *35*, 7427-7435, https://doi.org/10.1021/ma0204812.
38. Gohy, J.C.; Lohmeijer, B.G.G.; Varshney, S.K.; Décamps, B.; Leroy, E.; Boileau, S.; Schubert, U.S. Stimuli-Responsive Aqueous Micelles from an ABC Metallo-Supramolecular Triblock Copolymer. *Macromolecules*, **2002**, *35,* 9748-9755, https://doi.org/10.1021/ma021175r.
39. Mayer, G.; Vogel, V.; Lohmeijer, B.G.G.; Gohy, J.-C.; Van den Broek, J.A.; Haase, W.; Schubert, U.S.; Schubert, D. Metallo-supramolecular block copolymer micelles: Improved preparation and characterization. *J. Polym. Sci. Poly. Chem. Ed.* **2004**, *42,* 4458-4465, https://doi.org/10.1002/pola.20263.
40. Patil, A.O.; Schulz, D.N.; Novak, B.M. Functional polymers. Modern synthetic methods and novel structures. *ACS Symp Ser*. **1998,** *704.*
41. Hadjichristidis, N.; Pitsikalis, M.; Pispas, S.; Iatrou, H. Polymers with complex architectures by living anionic polymerization. *Chem. Rev.* **2001**, *101,* 3747-3792, https://doi.org/10.1021/cr9901337.
42. Hadjichristidis, N.; Hirao, A. Eds. *Anionic Polymerization. Principles, practice, strength, consequences and applications*. Springer Japan **2015**.
43. Hadjichristidis, N.; Pispas, S.; Pitsikalis, M. End-functionalized polymers with zwitterionic end-groups *Progr. Polym. Sci.* **1999**, *24*, 875-915, https://doi.org/10.1016/S0079-6700(99)00018-0
44. Borlenghi, A.; Pitsikalis, M.; Pispas, S.; Hadjichristidis, N. Association behavior of linear ω-functionalized polystyrenes in dilute solutions. *Macromol. Chem. Phys.* **1995**, *196*, 4025-4038, https://doi.org/10.1002/macp.1995.021961213.
45. Pitsikalis, M.; Siakali-Kioulafa, E.; Hadjichristidis, N. Association behavior of linear ω-functionalized polybutadienes in

cyclohexane. *J. Polym. Sci. Polym. Phys. Ed.* **1996**, *34*, 249-259, https://doi.org/10.1002/(SICI)1099-0488(19960130)34:2<249::AID-POLB5>3.0.CO;2-O.
46. Pispas, S.; Hadjichristidis, N. End Functionalized Block Copolymers of Styrene and Isoprene: Synthesis and Association Behavior in Dilute Solutions *Macromolecules* **1994**, *27*, 1891-1896, https://doi.org/10.1021/ma00085a035.
47. Pispas, S.; Hadjichristidis, N.; Mays, J. W. Association of End-Functionalized Block Copolymers. Light Scattering and Viscometric Studies *Macromolecules* **1994**, *27*, 6307-6317, https://doi.org/10.1021/ma00100a013.
48. Floudas, G.; Fytas, G.; Pispas, S.; Hadjichristidis, N.; Pakula, T.; Khokhlov, A.R. Statics and Dynamics of ω-Functionalized Block Copolymers of Styrene and Isoprene. *Macromolecules* **1995**, *28*, 5109-5118 https://doi.org/10.1021/ma00118a045.
49. Pitsikalis, M.; Hadjichristidis, N. Model mono-, di- and tri-ω-functionalized three arm star polybutadienes. Synthesis and association in dilute solution by membrane osmometry and static light scattering. *Macromolecules* **1995**, *28,* 3904-3910, https://doi.org/10.1021/ma00115a023.
50. Pitsikalis, M.; Hadjichristidis, N.; Mays, J.W. Model mono-, di- and tri-ω-functionalized three arm star polybutadienes. Association behavior in dilute solutions by dynamic light scattering and viscometry. *Macromolecules* **1996**, *29*, 179-184, https://doi.org/10.1021/ma951001s.
51. Siqueira, D.F.; Pitsikalis, M.; Hadjichristidis, N.; Stamm, M. Effect of chain-architecture on adsorption from dilute solution: ω-functionalized linear and mono-, di-, and tri-ω-functionalized three arm star polybutadienes. *Langmuir*, **1996**, *12*, 1631.
52. Vlassopoulos, D.; Fytas, G.; Pitsikalis, M.; Hadjichristidis, N.; Pakula, T. Controlling the self-assembly and dynamic response of star polymers by selective telechelic functionalization. *J. Chem. Phys.* **1999**, *111*, 1760-1764, https://doi.org/10.1063/1.479437.
53. Vlassopoulos, D.; Pitsikalis, M.; Hadjichristidis, N. Linear dynamics of end-functionalized polymer melts: linear chains, stars and blends *Macromolecules* **2000**, *33*, 9740-9746, https://doi.org/10.1021/ma000741k.
54. Charalabidis, D.; Pitsikalis, M.; Hadjichristidis, N. Model linear and star-shaped polyisoprenes with phosphatidylcholine analogous end-groups. Synthesis and association behavior in cyclohexane. *Macromol. Chem. Phys.* **2002**, *203*, 2132-2141, https://doi.org/10.1002/1521-3935(200210)203:14<2132::AID-MACP2132>3.0.CO;2-X.
55. Galland, D.; Belakhovsky. M.; Medrignac, F.; Pinéri, M. Microstructure of copper(II) α,ω-dicarboxylato polybutadiene *Polymer*, **1986** *27*, 883-888, https://doi.org/10.1016/0032-3861(86)90299-5.
56. Chujo, Y.; Saegusa, T. Cobalt(III) bipyridyl-branched polyoxazoline complex as a thermally and redox reversible hydrogel. *Macromolecules* **1993**, *26*, 6320-6323, https://doi.org/10.1021/ma00076a002
57. Chujo, Y.; Saegusa, T. Iron(II) bipyridyl-branched polyoxazoline complex as a thermally reversible hydrogel. *Macromolecules* **1993**, *26*, 6315-6319, https://doi.org/10.1021/ma00076a001.
58. Calzia, K.J.; Tew, G.N. Methacrylate polymers containing metal binding ligands for use in supramolecular materials: Random copolymers containing terpyridines. *Macromolecules* **2002**, *35*, 6090-6093, https://doi.org/10.1021/ma025551j.
59. Charlier, P.; Jerome, R.; Teyssie, P. Solution behavior of α,ω-(dimethylamino)polyisoprene coordinated to transition metal salts. *Macromolecules* **1990**, *23*, 1831-1837, https://doi.org/10.1021/ma00208a046.
60. Hadjichristidis, N.; Iatrou, H.; Pispas, S.; Pitsikalis, M. Anionic polymerization: High vacuum techniques. *J. Polym. Sci. Part A Polym. Chem.* **2000**, *38*, 3211-3234. https://doi.org/10.1002/1099-0518(20000915)38:18<3211::AID-POLA10>3.0.CO;2-L.
61. Uhrig, D.; Mays, J.W. Experimental techniques in high-vacuum anionic polymerization. *J. Polym. Sci., Part A: Polym. Chem.*, **2005**, *43*, 6179-6222, https://doi.org/10.1002/pola.21016.
62. Hadjichristidis, N.; Hirao, A. Eds. Chapter 1 page 3, Ratkanthwar, K.; Zhao, J.; Zhang, H.; Hadjichristidis, N.; Mays, J.W. *Anionic Polymerization. Principles, practice, strength, consequences and applications*. Springer Japan, **2015**.
63. Hadjichristidis, N., Hirao, A. Eds chapter 2, page 19, Ratkanthwar, K.; Hadjichristidis, N.; Mays, J.W. *Anionic Polymerization. Principles, practice, strength, consequences and applications*. Springer Japan, **2015**.
64. Hirao, A.; Hattori, I.; Sasagawa, T.; Yamaguchi, K.; Nakahama, S.; Yamazaki, N. Synthesis of polymers with primary amino end groups, 1. Reactions of anionic living polymers with protected aminating reagents. *Makromol. Chem. Rapid Commun.* **1982**, *3*, 59-63, https://doi.org/10.1002/marc.1982.030030111.
65. Ueda, K.; Hirao, K.; Nakahama, S. Synthesis of polymers with amino end groups. 3. Reactions of anionic living polymers with α-halo-ι-aminoalkanes with a protected amino functionality. *Macromolecules* **1990**, *23*, 939-945, https://doi.org/10.1021/ma00206a006.
66. Antonietti, M.; Heinz, S.; Schmidt, M.; Rosenauer, C. Determination of the Micelle Architecture of Polystyrene/Poly(4-vinylpyridine) Block Copolymers in Dilute Solution *Macromolecules* **1994**, *27*, 3276-3281, https://doi.org/10.1021/ma00090a021

Supporting Information

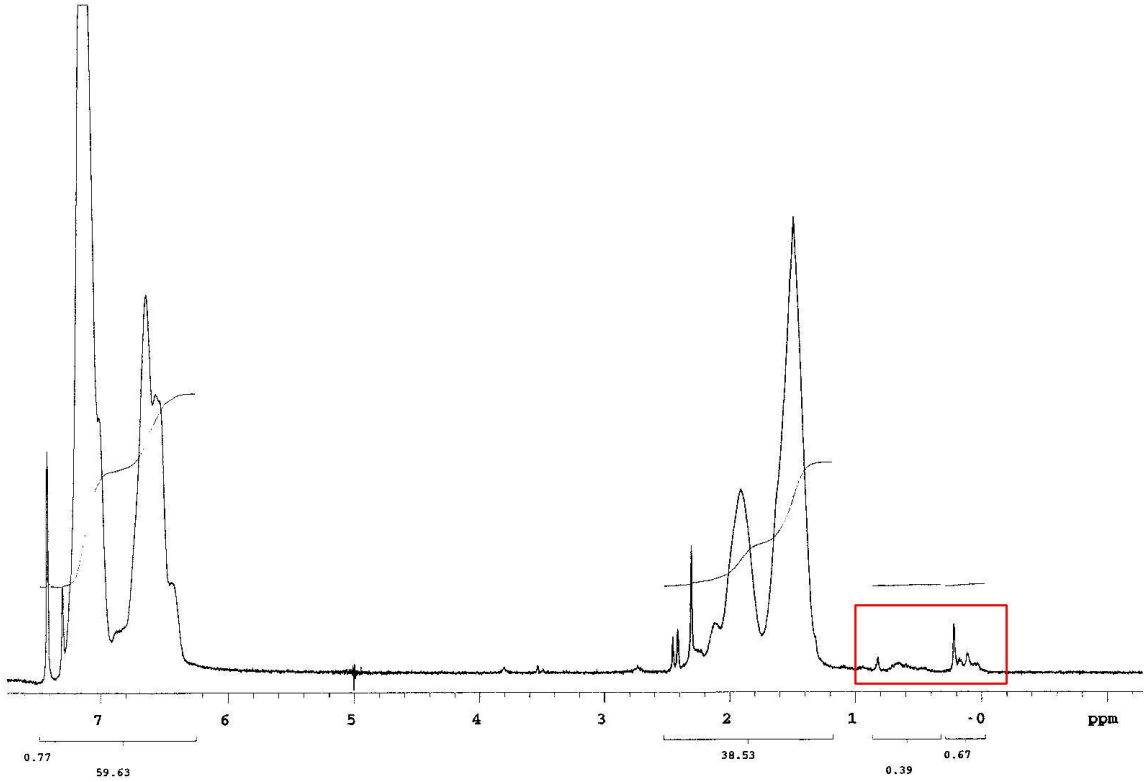

Figure SI 1a: ^{1}H NMR spectrum of the protected aminopolystyrene NPS8

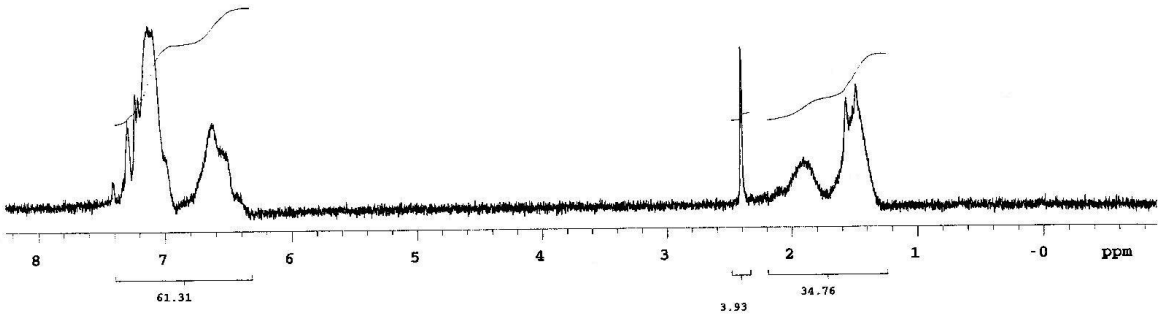

Figure SI 1b: ^{1}H NMR spectrum of the deprotected aminopolystyrene NPS8